

Analytical Methods

Accepted Manuscript



This is an *Accepted Manuscript*, which has been through the Royal Society of Chemistry peer review process and has been accepted for publication.

Accepted Manuscripts are published online shortly after acceptance, before technical editing, formatting and proof reading. Using this free service, authors can make their results available to the community, in citable form, before we publish the edited article. We will replace this *Accepted Manuscript* with the edited and formatted *Advance Article* as soon as it is available.

You can find more information about *Accepted Manuscripts* in the [Information for Authors](#).

Please note that technical editing may introduce minor changes to the text and/or graphics, which may alter content. The journal's standard [Terms & Conditions](#) and the [Ethical guidelines](#) still apply. In no event shall the Royal Society of Chemistry be held responsible for any errors or omissions in this *Accepted Manuscript* or any consequences arising from the use of any information it contains.

1
2
3 **One-Step determination of lead at higher level of linear range by artificial neural**
4 **network after Air-assisted liquid-liquid microextraction coupled to flame atomic**
5 **absorption spectrometry**
6
7
8
9

10
11
12
13
14
15
16
17
18 Gholamreza Fakhriyan, Hassan Zavvar Mousavi*, Sayedeh Maryam Sajjadi

19
20 Department of Chemistry, College of Science, Semnan University, Semnan, Iran, Zip Code:
21
22 35131-19111
23
24
25
26
27
28
29

30 * Corresponding Authors

31
32 Tel: +98 231 3366194

33
34 Fax: +98 231 3354110

35
36
37 E-Mail: hzmousavi@semnan.ac.ir
38
39
40
41
42
43
44
45
46
47
48
49
50
51
52
53
54
55
56
57
58
59
60

Abstract

A simple and rapid method was proposed for preconcentration of trace levels of lead prior to its determination by flame atomic absorption spectroscopy based on air-assisted liquid–liquid microextraction. Lead preconcentration was mediated by chelation with 4-(2-pyridylazo)resorcinol (PAR). Several variables affecting the method such as the pH of the sample, concentration of PAR, volume of extraction solvent and number of extraction cycles were investigated and optimized conditions were achieved. Under the optimum conditions, the calibration graph was linear in the range of 5-60 ng mL⁻¹. Limit of detection (LOD) and relative standard deviation (RSD %) for five replicate determinations (40 ng mL⁻¹) were 1.36 ng mL⁻¹ and 5.2%, respectively. Artificial neural network (ANN) strategy was used to extend the dynamic range (LDR) of the calibration, which prompted LDR to increase more than three folds (3-210 ng mL⁻¹) approximately. The root mean square of the percentage deviations (RMSPD) was 6.55%. This strategy was successfully applied to determine lead in water samples.

Keywords: Air-assisted liquid-liquid Microextraction, Preconcentration, LDR, Lead, ANN, Flame atomic absorption spectrometry

1. Introduction

Lead has been utilized throughout history and is widely distributed and globally mobilized. Although lead in the environment has been somewhat mitigated, but the nature of lead and its extensive uses in the past has prohibited it from being completely absent from our environment, and exposure to lead is still a public health concern.¹

Metals and their compounds in all living organisms play many significant roles. Nevertheless, when their exposure is excessive, they may cause toxic effects.² Therefore, we need to determine whether low-level environmental exposure to heavy metals which comes from the air, drinking water and food, can adversely affect pulmonary function in the general adult population.³

A variety of procedures have been developed for preconcentration of metals, such as solid phase extraction (SPE), liquid–liquid extraction (LLE), coprecipitation and cloud point extraction (CPE).⁴ However, disadvantages such as being time-consuming, unsatisfactory enrichment factors, the use of large amounts of organic solvents, and secondary wastes limit their applications.⁵

The development of sample pretreatment approaches involving minimization of solvent consumption and waste generation, as well as integration of steps is one of the main objectives pursued by the green analytical chemistry.⁶⁻¹⁴

Rezaee et al.¹⁵ introduced the technique of dispersive liquid–liquid microextraction (DLLME) for the extraction of organic compounds in 2006. DLLME consists of a miniaturization of the LLE, which results in a drastic reduction of the extraction phase volume (usually an organic solvent). In contrast, the presence of a disperser in DLLME reduces the polarity of aqueous phase that leads to increase the solubility of analytes into aqueous phase and decreases extraction

1
2
3 efficiency. In order to overcome to this problem, some disperser solvent-free techniques such as
4
5 ultrasound-assisted emulsification microextraction have been developed (USAEME).¹⁶
6
7

8 Farajzadeh and Mogaddam reported a novel version of DLLME called air-assisted liquid-
9
10 liquid microextraction (AALLME) to determine phthalate esters in aqueous samples.¹⁷ Flame
11
12 atomic absorption spectrometry (FAAS) was used, because it combines a fast analysis time, a
13
14 relative simplicity and lower costs.¹⁸ On the other hand, FAAS has short linear dynamic range for
15
16 some metals. Working outside the linear range may render inaccurate results,¹⁹ therefore, the
17
18 analyst is often forced to dilute a given sample in order to bring the analyte concentration within
19
20 the linear range. Besides being time-consuming, the latter poses the intrinsic risk of contaminating
21
22 the sample during the dilution process.
23
24
25
26

27 There are two strategies to solve the above inconvenience. The first one is experimental
28
29 approaches such as high-pressure atomizers,^{20, 21} quantitation at non-resonant absorption lines²²
30
31 non-stop gas condition during atomization.²³ The second strategy is applying mathematical models
32
33 such as polynomial expression²⁴ and artificial neural networks (ANN).²⁵
34
35

36 Modeling by means of an ANN represents an alternative calibration technique, for its use helps in
37
38 reducing sample manipulation (due to the extension of the working calibration range), and may
39
40 provide higher accuracy of the determinations in the non-linear portion of the curve (as a result of
41
42 the better fitness of the model).²⁶
43
44
45

46 In the present work, the first goal was quantification of lead in aqueous solutions in trace level
47
48 by AALLME coupled to flame atomic absorption spectrometry. In this purpose, the effective
49
50 parameters on the extraction efficiency such as volume of extraction solvent, pH, extraction time
51
52 and salt effect were investigated and the optimize conditions for the extraction were achieved.
53
54
55
56
57
58
59
60

1
2
3 Then, ANN was applied for pre-concentrated analyte, in the optimal condition, to enhance the
4
5 LDR of the calibration four folds approximately.
6
7
8
9

10 **2. Material and methods**

11 **2.1. Instrumentation**

12
13 An Agilent AA-200 (United States) equipped with deuterium background correction lamp was
14
15 used for the determination of lead. A lead hollow cathode lamp (Hamamatsu photonics, Shizuoka,
16
17 Japan) was used as the radiation source, operated at 10 mA with monochromator spectral band
18
19 pass of 0.2 nm and 217.0 nm wavelength. Measurements were carried out in the peak height mode
20
21 with air-acetylene flame. An EBA20 model centrifuge (Hettich, Germany) was used to accelerate
22
23 phase separation. A home-made micro-sample introduction system was used for injection of the
24
25 extraction phase in flame atomic absorption spectrometry and a metrohm 632 pH-meter (Herisau,
26
27 Switzerland) equipped with a glass combination electrode was employed for adjusting the pH of
28
29 the solutions.
30
31
32
33
34
35

36 A glass syringe was used for suction step. A Pentium computer performed the Data processing.
37
38 The authors use the ANN toolbox algorithms in MATLAB software (Math Work, R2013B).
39
40
41
42

43 **2.2. Reagents and sample solution**

44
45 Acids, bases and organic solvents were of the highest purity available from Merck (Darmstadt,
46
47 Germany). Nitrate salts of all metal ions including analytes and interferences were purchased from
48
49 Merck, and were used without any further purification.
50
51
52

53 All solutions were prepared with deionized water. The lead stock solution (1000 mg L⁻¹) was
54
55 purchased from Merck. The working standard solutions were obtained by appropriate dilution of
56
57
58
59
60

1
2
3 the stock standard solutions. The chelating agent, 4-(2-pyridylazo) resorcinol (PAR) was
4 purchased from Merck Company. Carbon tetrachloride with 99.5% purity was used as extraction
5 solvent. The primary pH of the samples was adjusted using 0.1 mol L⁻¹ hydrochloric acid or 0.1
6 mol L⁻¹ sodium hydroxide. The pH of sample solutions was adjusted with the phosphate buffer
7 solutions.
8
9

10 11 12 13 14 15 **2.3. Extraction procedure**

16
17 10 mL solution of Pb (II) and PAR (3.64×10^{-4} mol L⁻¹) in deionized water was adjusted at pH
18 6.5 and transferred into a conical bottom glass centrifuge tube. Then 210 μ L CCl₄ was added to the
19 tube. The mixture was rapidly sucked into a 10-mL glass syringe and then was injected into the
20 tube. The procedure was repeated for seven times via syringe needle. To prevent the memory
21 effect, glass syringe was washed with acetone and distilled water before performing the next
22 microextraction experiment. The cloudy solution was centrifuged for 4 min at 4000 rpm. After
23 withdrawing of the upper solution, 100 μ L from the fine droplets of CCl₄ settled in the bottom of
24 the tube was removed by ependorf micropipette and aspirated to flame atomic absorption
25 spectrometry at peak area mode.
26
27
28
29
30
31
32
33
34
35
36
37
38
39
40

41 42 43 **3. Results and Discussion**

44 In this study, preconcentration of trace level of lead under air assisted liquid-liquid
45 microextraction was performed. A number of parameters such as type and volume of extracting
46 solvent, pH, chelating agent concentration and extraction time were investigated and the optimum
47 conditions of lead extraction were obtained. Then ANN was applied to enhance the LDR of the
48 concentration.
49
50
51
52
53
54
55
56
57
58
59
60

3.1. Investigation of effective parameters on the extraction efficiency

3.1.1 Extraction solvent type

Selecting an appropriate extraction solvent is serious in the AALLME process to achieve high extraction efficiency. In this type of AALLME, extraction solvent must have properties such as being denser than water, low background in resonance line and high extraction capability for the target analyte. In this work, 150 microliter of CCl_4 , CHCl_3 and Chlorobenzene were used as extraction solvent and their efficiencies were compared. As it could be seen from Figure 1, CCl_4 has the highest performance in extraction of the lead complex due to its lowest polarity, therefore, this solvent was selected as the optimum extraction solvent.

<Fig. 1>

3.1.2. Extraction solvent volume

Experiments were performed with different volumes of carbon tetrachloride. Figure 2 indicates that, in the range 150-210 μL of the solvent volume, the more solvent volume, the more the absorbance but no further increase in the absorbance was observed above 210 μL , so, 210 μL of CCl_4 was chosen as the optimized extraction solvent volume.

<Fig. 2>

3.1.3 Effect of pH

The pH plays a unique role on metal-chelate formation and is an important factor for a hydrophobic complex formation for migration from aqueous solution to organic solution. The separation and preconcentration of metal ions by AALLME involve a prior formation of metal-chelate with enough hydrophobicity and subsequent extraction into the small volume of the

1
2
3 sediment phase. Based on Figure 3, the maximum absorbance was obtained at pH 6.0 and this pH
4 was selected as the optimum value. At lower pH values, 6.0 the chelating agent is protonated and
5 its bonding sites to metal ions are limited which causes decrease in the recovery, while increase in
6 pH facilitates the metal ions to hydrolyze, which again decreases the extraction recovery.
7
8
9
10
11

12 <Fig. 3>
13
14
15
16
17

18 **3.1.4. Effect of PAR concentration**

19
20 Since Metal ions have high charge to surface ratio, their absorption by extraction solvent is
21 very low. Using a chelating agent, hydrophilic metal ions can be converted to hydrophobic
22 compounds. Here, the influence of PAR concentration, as a chelating agent, on the AALLME
23 extraction efficiency of Pb (II) ion was evaluated. The results showed that the absorbance
24 increased up to 3.64×10^{-4} mol L⁻¹ of PAR and leveled off at higher concentrations. Thus, $3.64 \times$
25 10^{-4} mol L⁻¹ ligand was selected as its optimum concentration.
26
27
28
29
30
31
32
33
34
35

36 **3.1.5. Extraction time**

37
38 In the AALLME method, the extraction time is described as the number of repeated procedure
39 to withdraw and push out the mixture of the aqueous sample solution and the extraction solvent
40 with a glass syringe into the conical test tube. Clearly, the extraction time plays an important role
41 in obtaining the highest extraction efficiency with the least time. In this section, the extraction
42 times were investigated in the range of 4–10 min. As the results in Figure 4 show, by increasing
43 the number of extraction cycles up to seven, the responses of the target analyte was increased and
44 then remained constant. Consequently, 8 cycles was selected for further studies. It is noted that this
45 step could be performed in <1 min, which would exhibit the speed of the suggested method.
46
47
48
49
50
51
52
53
54
55
56
57
58
59
60

<Fig. 4>

3.1.6. Centrifuge time and speed

Centrifugation time is another important factor that influences the separation of organic and aqueous phases. The centrifugation time was studied in the range of 1 - 6 min at the speed of 2000 - 4000 rpm. By considering the minimum of time and maximum of signal, 4 min and 4000 rpm were selected as the optimum conditions.

3.1.7. Effect of ionic strength

Generally, adding salt can decrease the solubility of the analytes in the aqueous phase and promote their transfer to the organic phase because of the salting out effect, thereby improving the extraction efficiency²⁴. However, when ionic strength increases, with decreasing the performance of mass-transfer process, the solution viscosity increases subsequently.

Various experiments were performed by adding different amounts of NaCl in the range of 0.1-0.5 mol L⁻¹ while the other parameters were kept constant. The results showed that the increasing of the salt concentration did not have effect on the extraction of lead.

3.1.8 Effect of coexisting ions

In order to demonstrate the selectivity of the developed microextraction system, the effect of different ions on lead determination was evaluated and the results are summarized in Table 1. The tolerance limit of foreign ions was taken as that value which caused an error of not more than $\pm 5\%$ in the absorbance. The ions normally present in water do not interfere under the experimental conditions used. Some of the transition metals were not interfered on the recoveries of the analyte

ions. Common anions such as nitrate, sulfate and acetate at high concentration have the ability to bind with metal ions. Therefore, in their presence the efficiency of the extraction may be reduced. To eliminate of these ions, we can use some adsorbents with positive surface charge, ion exchange or biologic method prior to AA-LLME. The results show that the proposed method could be applied for determination of lead in real samples.

<Table. 1>

3.2. Increasing the working range for the determination of lead by AAN

3.2.1. Artificial neural network theory

In artificial neural network (ANN), there are several neurons which are tightly connected in various layers. There are three types of layers: input, output and hidden layers sandwiched between the input layer and output layer. The hidden layers play a substantial role on the predicting ability of the developed ANN and the complexity of the problems determines the number of essential layers.

In ANN algorithm, each connector neuron between input and hidden layer has a value termed "weight (w)", performs a series of simple calculations. First, the input variables (X_i) are coded between -1 and +1 and processed in the "body" of the neuron according to:

$$z_i = \sum_{i=1}^n w_i x_i \quad (1)$$

Where w_i , the weights, represent the "artificial synapses". This value is further modified in a second step by means of a transfer function (Γ)²⁶. The outputs are computed via the neurons by processing the sum of weighted inputs through their transfer functions. A learning procedure tries

1
2
3 to find a set of connections w 's that gives a mapping that fits the training set well.²⁷ Here, *trainlm*
4
5 was selected as a network training function that updates weights according to the Levenberg-
6
7 Marquardt optimization.²⁸
8
9

10
11
12 In the learning step of ANN algorithm, three sets of data must exist including training, testing
13 set and validation sets. Training set is used to adjust the weights on the neural network; set is used
14
15 to overcome over fitting. If the accuracy over the training data set increases, but the accuracy over
16
17 the test data set doesn't change or decreases, then the training should stop because of over fitting.
18
19 Validation set is used only for testing the final solution in order to confirm the actual predictive
20
21 power of the network.
22
23
24
25
26
27
28

29 **3.2.2. Optimization of neural network**

30
31 The main network parameters in matlab toolbox such as topology, number of data in each
32 category (training subset, validation subset and test subset) and training algorithm were introduced
33
34 in Table 2.
35
36
37

38 <Table. 2>
39
40
41
42

43 The initial weights of inputs and bias were estimated randomly. In order to avoid the dependency
44 of the training of ANN to initial weights, the network was trained for 100 times.
45
46
47

48 To evaluate the training step and find the topology of the ANN model, two statistical
49 parameters such as mean square error (MSE) and correlation coefficient were used, which are
50
51 defined as follows:
52
53
54

$$55 \quad MSE = \frac{\sum_i (y_{pred,i} - y_{exp,i})^2}{n} \quad (2)$$

56
57
58
59
60

$$R^2 = 1 - \frac{\sum_i (y_{pred,i} - y_{exp,i})^2}{\sum_i (y_{pred,i} - y_m)^2} \quad (3)$$

Where $y_{pred,i}$, $y_{exp,i}$ are the i th predicted value of lead concentration from ANN and its corresponding real experimental value, respectively. Subscribe y_m is the mean of y_{exp} . The changing of MSE with respect to epoch (iteration) numbers is depicted in Figure 5.

<Fig. 5>

While a reduction of the MSE is an important aspect to be considered for selecting the most adequate topology, it is as relevant evaluating the generalization capacity with data not used during the training process. The optimal ANN structure model was determined based on the maximum value of R^2 and the minimum value of the MSE of the testing set. Here, (1×3×1) network was the optimal model whose topology and regression coefficients were depicted in Figure 6 and Figure 7.

<Fig. 6>

<Fig. 7>

The regression equation of Pb for this model was $[Pb]_{Pred} = 1 * [Pb]_{Real} + 0.00016$ ($R^2 = 0.99884$). A Student's t-test showed that the intercept and the slope of such equations did not differ significantly ($P = 0.05$) from 0 and 1, respectively, indicating the adequacy of the model in a first approximation. The goodness-of-fit of the model generated by the ANN was assessed through the estimation of the root mean square of the percentage deviations (RMSPD)²⁹

$$RMSPD = \left(\frac{1}{N} \sum_{i=1}^N \left(\frac{C_{pred} - C_{real}}{C_{real}} \times 100 \right)^2 \right)^{\frac{1}{2}} \quad (4)$$

Where C_{pred} and C_{real} matches to the i th predicted and actual concentrations of lead, respectively, and N is the number of points used in the calibration. The calculated RSMPD was 6.55% that was a clear indication of the capability of the neural network for modeling the calibration curve in the

1
2
3 whole range of the study. Based on Figure 8, in the higher numerical concentration of lead,
4
5 RMSPD has increased dramatically. Thus, the working range 3-210 ng mL⁻¹ was selected as
6
7 optimum working range that it was demonstrated an increase in the range compare to primary
8
9 linear range 5-60 ng mL⁻¹.
10
11

12 <Fig. 8>
13
14
15
16
17

18 3.3. Analytical features

19 3.3.1. Figures of merit

20 The classical calibration graph for the mentioned procedure was plotted. Under the optimized
21
22 conditions, the calibration graph was linear in the range of 5-60 ng mL⁻¹ when using of 10 mL
23
24 sample solution. After using of ANN for prediction of concentration, the working range was
25
26 obtained 3-210 ng mL⁻¹. The limit of detection (LOD) was 1.36 ng mL⁻¹ based on 3s_b (three times
27
28 of standard deviation of blank solution). The relative standard deviation (RSD) for five replicates
29
30 analysis of 30 ng mL⁻¹ Pb²⁺ was 5.14%. The enrichment factor was calculated from the slope ratio
31
32 of two calibration lines: before and after the preconcentration step. This factor was 58 without
33
34 using of ANN. As mentioned previously, the linear region for determination of lead in FAAS for
35
36 presented method is very low. For investigation of relative errors, comparison between spiked
37
38 value (20, 30 and 40 µg L⁻¹) in Table 3 demonstrated that the results did not have difference in
39
40 linear region but relative standard deviation in traditional method was higher than ANN. This fact
41
42 may be performed from successive dilutions or difference in matrices properties.
43
44
45
46
47
48
49
50
51

52 <Table. 3>
53
54
55
56
57
58
59
60

3.3.2. Comparison of proposed procedure with other methods

The LOD, RSD and enrichment factor for different methods on preconcentration and determination of lead by flame atomic absorption spectrometry are given in Table 4 and are compared with the present work. The results demonstrate that AALLME-FAAS is a sensitive method for preconcentration and determination of lead. However, the RSD for determination of lead is as well as other presented methods approximately.

<Table. 4>

3.3.3 Analytical application

For validation of method, the proposed method was applied to determine Pb^{2+} ions in deionized water and natural water samples (tap water obtained from our laboratory, river water from Neyshabour, well water from Mashhad) within and without of linear range. The results were demonstrated in Table 5.

The percentage recovery (R) was determined by using of the equation: $R=100(C_s-C_0)/m$ where C_s is a value of metal in a spiked sample, C_0 is a value of metal in a sample and m is an amount of spiked metal. These results illustrated that the proposed procedure could be satisfactorily used for the analysis of water samples.

<Table. 5>

3.3.4 Accuracy of the Method

In order to investigate the accuracy and validity of the presented procedure, the method was applied to determination of lead in a Geochemical Reference Samples (GRS) in type JR-1. A 1.0 gram JR-1 certified reference material was dissolved in 10 mL of mixture of HNO_3 and HCl with concentration 3, 5 mol L^{-1} respectively. The solution was heated to near dryness and then it was

1
2
3 diluted to 100 mL with deionized water. The resultant solution was analyzed according to the
4
5 proposed method. As can be seen at Table 6, It was found that analytical results were in good
6
7 agreement with the certified values , no significant differences were observed (t test, p 0.05). It
8
9 indicates that the proposed procedure was helpful for the determination of Pb in the real samples
10
11 with complex matrices.
12
13

14
15 <Table. 6>
16

17 18 **4. Conclusions**

19
20 AALLME was developed for determination of lead in real samples with relative low LOD and
21
22 high enrichment factor but it has low linear range for determination of lead under mentioned
23
24 condition. An ANN was successfully used for modeling the calibration graph and increasing the
25
26 working range for lead. The procedure was simple, fast and sensitive and could be further
27
28 improved using graphite furnace atomic absorption spectrometry. The RSD of determination was
29
30 relatively high compared to other techniques. This may be due to the rapid attainment of
31
32 equilibrium. Combining ANN and AALLME showed a wide linear range for more than three
33
34 folds. This combination can reduce successive dilution steps.
35
36
37
38
39
40

41 42 **Acknowledgements**

43
44 The authors wish to thank Semnan University Research Council for financial support of this work.
45
46
47
48
49
50
51
52
53
54
55
56
57
58
59
60

References

1. N. M. Roy, S. DeWolf and B. Carneiro, *Aquat. Toxicol*, 2015, **158**, 138-148.
2. M. Janicka, Ł. J. Binkowski, M. Błaszczuk, J. Paluch, W. Wojtaś, P. Massanyi and R. Stawarz, *J. Trace Elem. Med Biol*, 2015, **29**, 342-346.
3. H. K. Chung, Y. S. Chang and C. W. Ahn, *Environ. Res*, 2015, **136**, 274-279.
4. R. Khani, F. Shemirani and B. Majidi, *Desalination*, 2011, **266**, 238-243.
5. A. Sarafraz-Yazdi, A. Amiri, G. Rounaghi and H. E. Hosseini, *J. Chromatogr. A*, 2011, **1218**, 5757-5764.
6. L. Li, B. Hu, L. Xia and Z. Jiang, *Talanta*, 2006, **70**, 468-473.
7. D. Afzali, A. R. Mohadesi, M. Falahnejad and B. Bahadori, *J. AOAC Int*, 2013, **96**, 161-165.
8. H. Jiang, Y. Zhang, B. Qiu and W. Li, *CLEAN–Soil, Air, Water*, 2012, **40**, 438-443.
9. H. Bai, Q. Zhou, G. Xie and J. Xiao, *Talanta*, 2010, **80**, 1638-1642.
10. F. Shah, T. G. Kazi, H. I. Afridi and M. Soylak, *Microchem. J*, 2012, **101**, 5-10.
11. S. Mohammadi, T. Shamspur and Y. Baghelani, *B. Chem. Soc. Ethiopia*, 2013, **27**, 161-168.

- 1
2
3
4
5
6
7
8
9
10
11
12
13
14
15
16
17
18
19
20
21
22
23
24
25
26
27
28
29
30
31
32
33
34
35
36
37
38
39
40
41
42
43
44
45
46
47
48
49
50
51
52
53
54
55
56
57
58
59
60
12. D. Afzali, M. Fayazi and A. FAVI, *J. Chilean Chem. Soc*, 2013, **58**, 1593-1596.
 13. F. Shah, E. Yilmaz, T. G. Kazi, H. I. Afridi and M. Soylak, *Analytical Methods*, 2012, **4**, 4091-4095.
 14. M. T. Naseri, M. R. M. Hosseini, Y. Assadi and A. Kiani, *Talanta*, 2008, **75**, 56-62.
 15. M. Rezaee, Y. Assadi, M.-R. Milani Hosseini, E. Aghaee, F. Ahmadi and S. Berijani, *J. Chromatogr. A*, 2006, **1116**, 1-9.
 16. J. Regueiro, M. Llompert, C. Garcia-Jares, J. C. Garcia-Monteagudo and R. Cela, *J. Chromatogr. A*, 2008, **1190**, 27-38.
 17. M. A. Farajzadeh and M. R. A. Mogaddam, *Analytica Chimica Acta*, 2012, **728**, 31-38.
 18. S. Z. Mohammadi, D. Afzali, M. A. Taher and Y. M. Baghelani, *Talanta*, 2009, **80**, 875-879.
 19. J. M. M. Gayon, A. Sanz-Medel, C. Fellows and P. Rock, *J. Anal. At. Spectrom*, 1992, **7**, 1079-1083.
 20. R. E. Sturgeon, C. L. Chakrabarti and P. C. Bertels, *J. Anal. Chem*, 1975, **47**, 1250-1257.
 21. R. E. Sturgeon, C. L. Chakrabarti and P. C. Bertels, *Spectrochim. Acta. B*, 1977, **32**, 257-277.
 22. M. A. Belarra, M. Resano and J. R. Castillo, *Spectrochim. Acta. B*, 1996, **51**, 697-705.
 23. J. B. B. da Silva, M. B. I. O. Giacomelli, I. G. de Souza and A. J. Curtius, *Anal. Chim. Acta*, 1999, **401**, 307-315.
 24. L. He, X. Luo, H. Xie, C. Wang, X. Jiang and K. Lu, *Anal. Chim. Acta*, 2009, **655**, 52-59.
 25. H. C. Wagenaar and L. de Galan, *Spectrochim. Acta. B*, 1975, **30**, 361-381.
 26. E. A. Hernández-Caraballo, R. M. Avila-Gómez, F. Rivas, M. Burguera and J. L. Burguera, *Talanta*, 2004, **63**, 425-431.

- 1
2
3
4
5
6
7
8
9
10
11
12
13
14
15
16
17
18
19
20
21
27. H. Taghavifar, A. Mardani, A. Mohebbi and H. Taghavifar, *Fuel*, 2014, **137**, 1-10.
 28. D. W. Marquardt, *J. Soc. Ind. Appl. Math*, 1963, **11**, 431-441.
 29. N. J. Miller-Ihli, T. C. O'Haver and J. M. Harnly, *Spectrochim. Acta. B*, 1984, **39**, 1603-1614.
 30. C. Karadaş and D. Kara, *J. Food. Compos. Anal*, 2013, **32**, 90-98.
 31. S. Candir, I. Narin and M. Soylak, *Talanta*, 2008, **77**, 289-293.
 32. M. T. Naseri, P. Hemmatkhah, M. R. M. Hosseini and Y. Assadi, *Anal. Chim. Acta*, 2008, **610**, 135-141.

Figure captions

22
23
24
25
26
27
28
29
30
31
32
33

Fig. 1 The effect of extraction solvent type on the absorbance of lead, concentration Pb (II) 30.0 ng mL⁻¹, pH=8, PAR=4.0 × 10⁻⁵ mol L⁻¹, centrifuge time 5 min, cycle=10

Fig. 2 The effect of the volume of extraction solvent on the absorbance of Pb (II), lead 30 ng mL⁻¹, PAR= 4.0 × 10⁻⁵ mol L⁻¹, centrifuge time 5 min, cycle=10

Fig. 3 The effect of pH on the absorbance of lead, concentration Pb (II) 30.0 ng mL⁻¹, PAR: 4.0 × 10⁻⁵ mol L⁻¹, CCl₄ : 210 µl, centrifuge time: 5 min, cycle=10

Fig. 4 The effect of the number of extraction cycles on the absorbance of lead, lead 40 ng mL⁻¹, PAR= 3.63 × 10⁻⁴ mol L⁻¹, CCl₄ (210 µl), pH=6.5, centrifuge time 5 min.

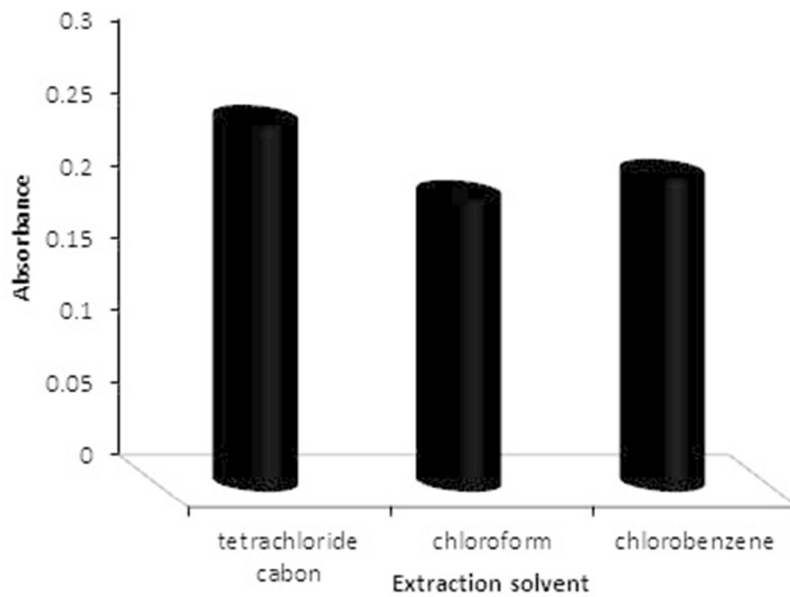
Fig. 5 The neural network diagram

Fig. 6 The MSE reduction with the increase in epochs numbers owing to the back-propagation algorithm

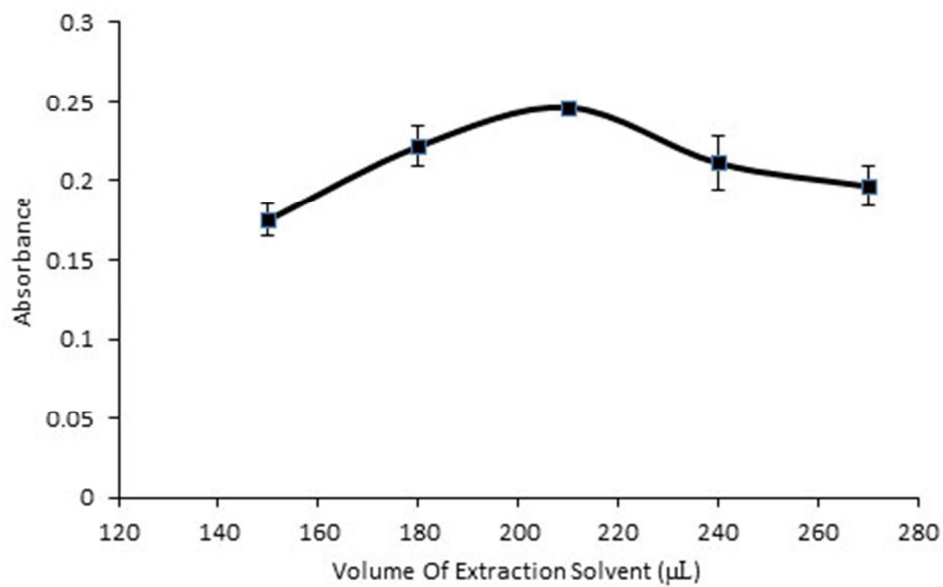
Fig. 7 The scatterplots of developed data (target) versus ANN predicted model (output) for training, validation, and testing phases.

Fig. 8 The increasing in RMSPD at wider calibration range.

1
2
3
4
5
6
7
8
9
10
11
12
13
14
15
16
17
18
19
20
21
22
23
24
25
26
27
28
29
30
31
32
33
34
35
36
37
38
39
40
41
42
43
44
45
46
47
48
49
50
51
52
53
54
55
56
57
58
59
60



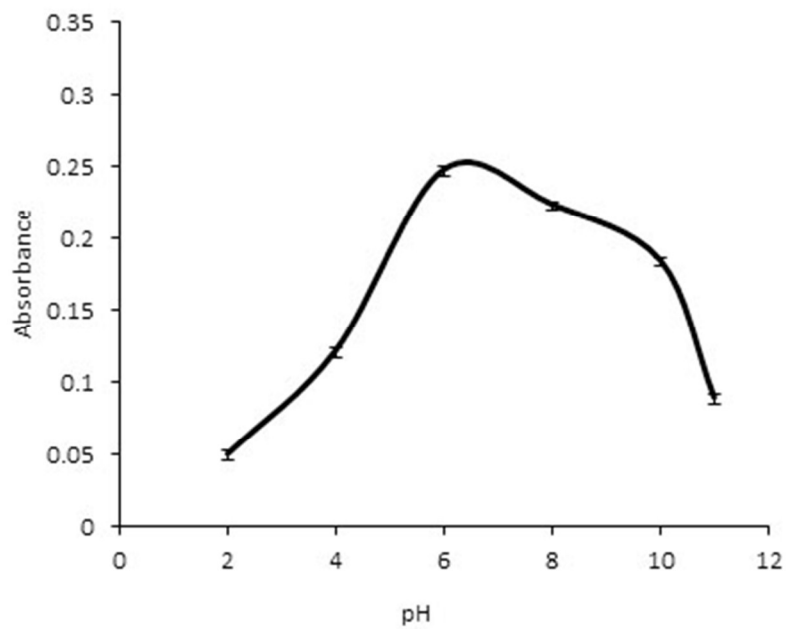
169x112mm (72 x 72 DPI)



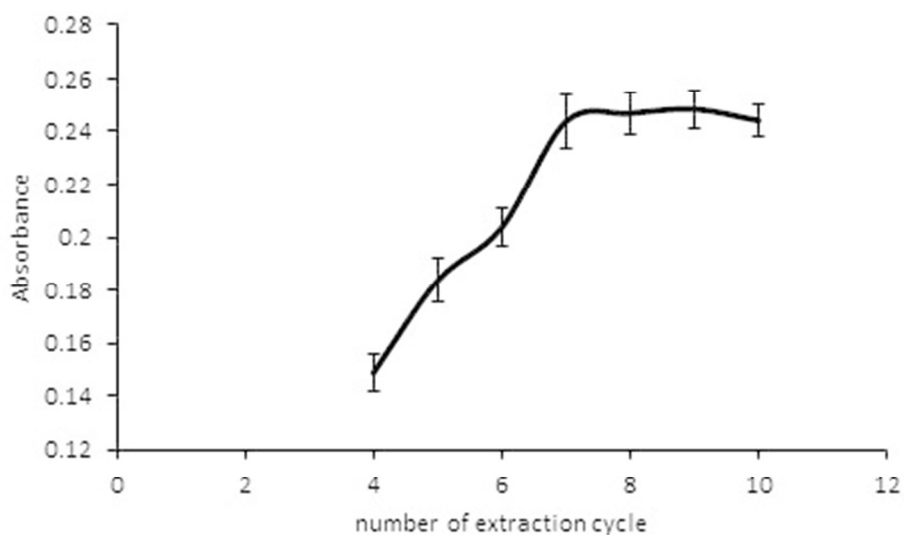
175x110mm (72 x 72 DPI)

1
2
3
4
5
6
7
8
9
10
11
12
13
14
15
16
17
18
19
20
21
22
23
24
25
26
27
28
29
30
31
32
33
34
35
36
37
38
39
40
41
42
43
44
45
46
47
48
49
50
51
52
53
54
55
56
57
58
59
60

1
2
3
4
5
6
7
8
9
10
11
12
13
14
15
16
17
18
19
20
21
22
23
24
25
26
27
28
29
30
31
32
33
34
35
36
37
38
39
40
41
42
43
44
45
46
47
48
49
50
51
52
53
54
55
56
57
58
59
60



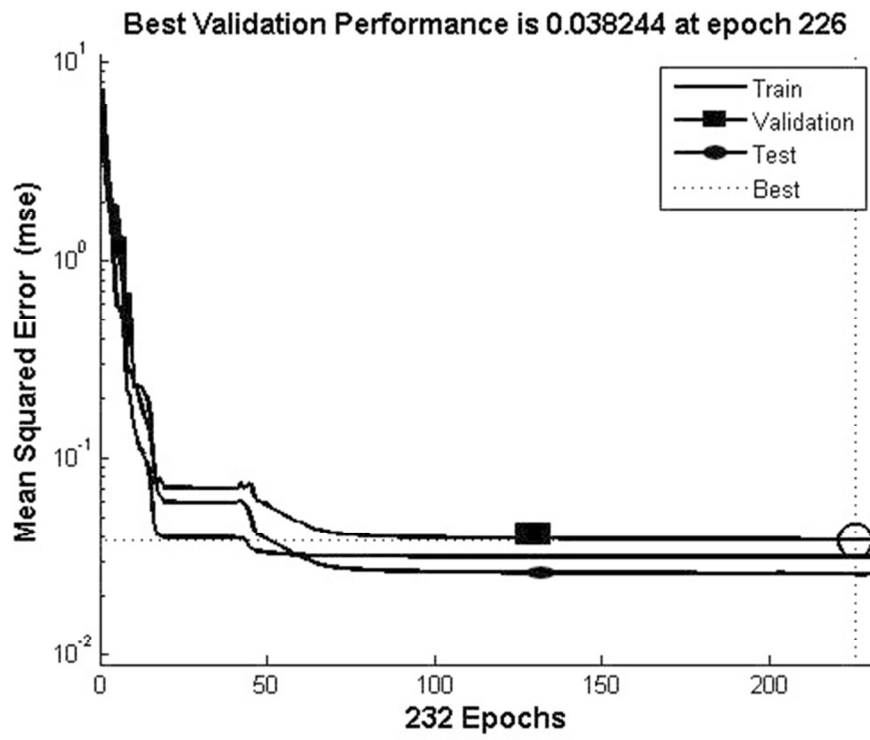
169x117mm (72 x 72 DPI)



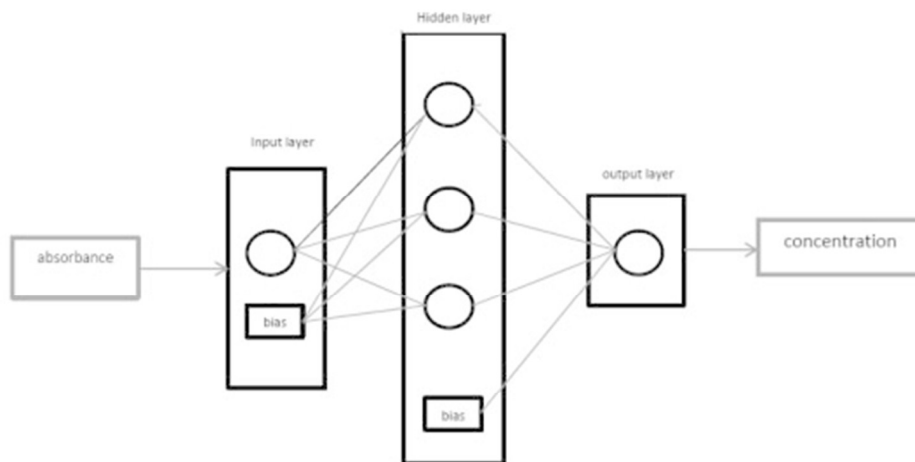
169x101mm (72 x 72 DPI)

1
2
3
4
5
6
7
8
9
10
11
12
13
14
15
16
17
18
19
20
21
22
23
24
25
26
27
28
29
30
31
32
33
34
35
36
37
38
39
40
41
42
43
44
45
46
47
48
49
50
51
52
53
54
55
56
57
58
59
60

1
2
3
4
5
6
7
8
9
10
11
12
13
14
15
16
17
18
19
20
21
22
23
24
25
26
27
28
29
30
31
32
33
34
35
36
37
38
39
40
41
42
43
44
45
46
47
48
49
50
51
52
53
54
55
56
57
58
59
60

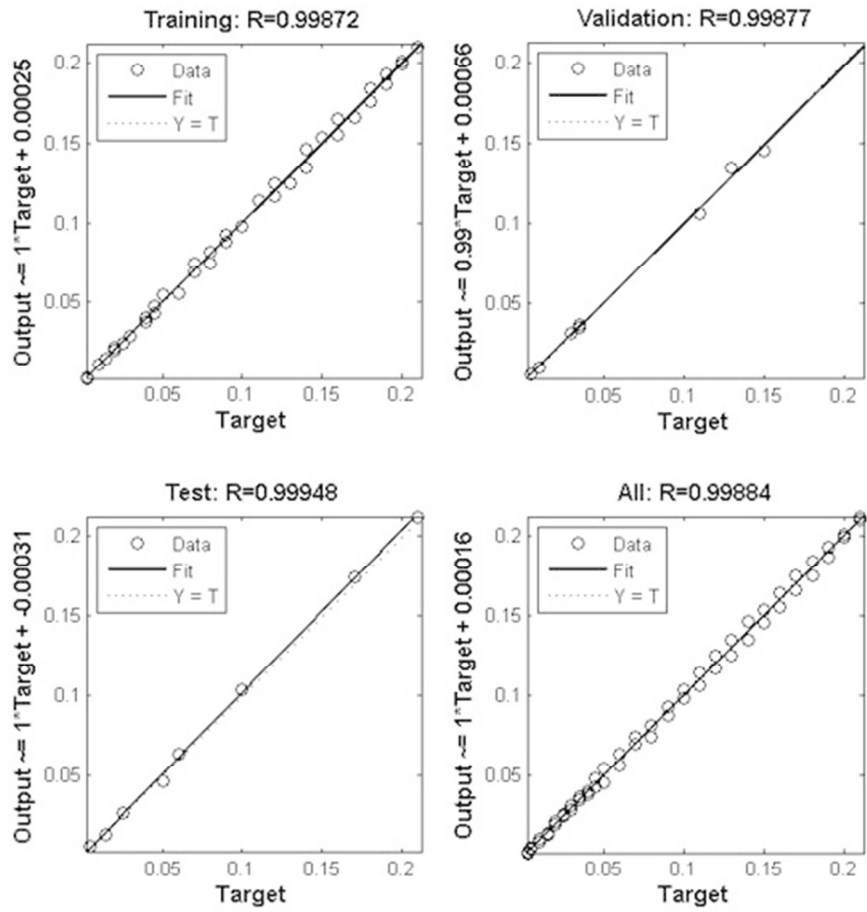


197x148mm (72 x 72 DPI)



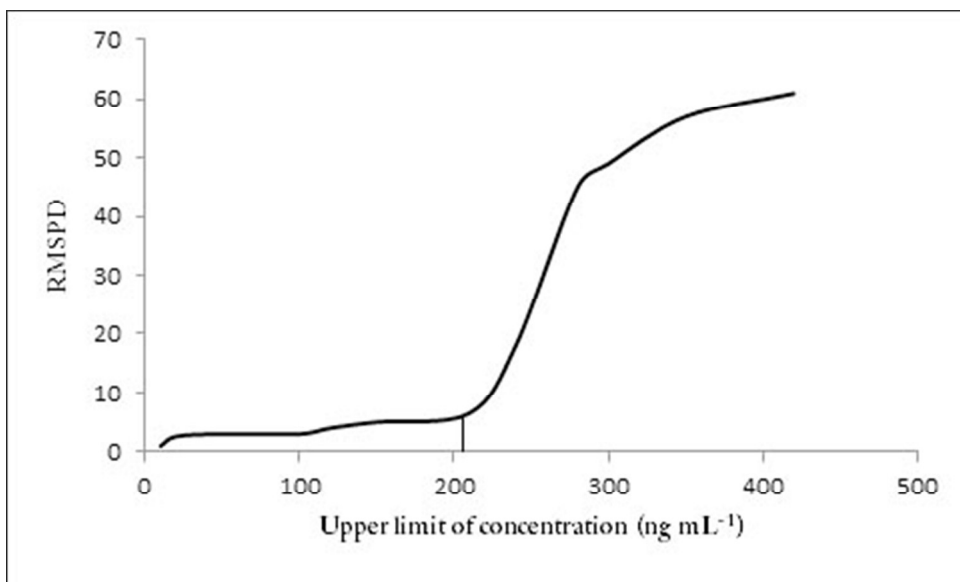
203x100mm (72 x 72 DPI)

1
2
3
4
5
6
7
8
9
10
11
12
13
14
15
16
17
18
19
20
21
22
23
24
25
26
27
28
29
30
31
32
33
34
35
36
37
38
39
40
41
42
43
44
45
46
47
48
49
50
51
52
53
54
55
56
57
58
59
60



220x220mm (72 x 72 DPI)

1
2
3
4
5
6
7
8
9
10
11
12
13
14
15
16
17
18
19
20
21
22
23
24
25
26
27
28
29
30
31
32
33
34
35
36
37
38
39
40
41
42
43
44
45
46
47
48
49
50
51
52
53
54
55
56
57
58
59
60



169x101mm (72 x 72 DPI)

1
2
3
4
5
6
7
8
9
10
11
12
13
14
15
16
17
18
19
20
21
22
23
24
25
26
27
28
29
30
31
32
33
34
35
36
37
38
39
40
41
42
43
44
45
46
47
48
49
50
51
52
53
54
55
56
57
58
59
60

Table. 1 Effect of interfere on the recovery 20 $\mu\text{g.L}^{-1}$ Pb (II) in water sample using AALLME-FAAS

| Interferent | Mass ratio Interfering ion/ Pb (II) | Recovery (%) |
|---------------------------|----------------------------------------|-----------------|
| NO_3^- | 1000 | 95.0 |
| Cl^- | 1000 | 97.0 |
| SO_4^{2-} | 1000 | 94.2 |
| CH_3COO^- | 1000 | 94.8 |
| Na^+ | 1000 | 99.0 |
| Ba^{2+} | 1000 | 102.5 |
| K^+ | 1000 | 98.1 |
| Mg^{2+} | 1000 | 98.0 |
| NH_4^+ | 1000 | 98.3 |
| Cr^{3+} | 400 | 96.1 |
| Ca^{2+} | 250 | 97.2 |
| Ag^+ | 100 | 95.7 |
| Ni^{2+} | 100 | 95.4 |
| Fe^{2+} | 50 | 96.2 |

Table .2 The network parameters in matlab toolbox

| | |
|--------------------------|------------------------------------------------------------------------------------------------------------------------------------------------------------------------------------------------------------------|
| Topology | 3 inputs, 1 outputs and 1 hidden layers with 4 hidden neurons (1-3-1) |
| data | Training subset: 70% randomly selected observation data (38 data) Validation subset: 15% randomly selected observation data (8 data) Test subset: 15% randomly selected observation data (8 data) |
| Beginning function | Log-sigmoid |
| Training algorithm | Levenberge Marquardt |
| Loss function conditions | Minimum MSE |
| Stopping conditions | The network stop in one of three way: 1: the validation check > 9 2: minimum gradient $< 10^{-7}$ 3: momentum speed $> 10^{10}$ |

1
2
3
4
5
6
7
8
9
10
11
12
13
14
15
16
17
18
19
20
21
22
23
24
25
26
27
28
29
30
31
32
33
34
35
36
37
38
39
40
41
42
43
44
45
46
47
48
49
50
51
52
53
54
55
56
57
58
59
60

Table. 3 Comparison of models for prediction of lead

| Concentration(ng mL ⁻¹) | Linear range | ANN |
|-------------------------------------|--------------|-----------|
| 20 | 19.0±1.1* | 19.2±1.2 |
| 30 | 32.4±2.1 | 31.1±1.6 |
| 40 | 41.20±2.9 | 41.10±2.1 |
| 60 | - | 63.1±3.8 |
| 90 | - | 94.2±5.5 |
| 110 | - | 118±5.9 |
| 130 | - | 139±7.2 |
| 150 | - | 146±9.1 |

* Values correspond to the average ± standard deviation ($N = 5$)

Table. 4 Comparison between presented method with other methods

| Method | LOD (ng mL ⁻¹) | RSD (%) | EF ^a | LDR ^b | WR ^c | Ref. |
|--------|----------------------------|---------|-----------------|------------------|-----------------|------------|
| SPE | 2.89 | 3.21 | 17.9 | 20-350 | LDR | 30 |
| CPE | 7.2 | <6 | - | 2-12 | LDR | 31 |
| DLLME | 0.5 | 3.8 | 450 | 1-70 | LDR | 32 |
| AALLME | 1.36 | 5.1 | 58 | 3-54 | 3-210 | This study |

a. Enrichment Factor

b. Linear dynamic range (ng mL⁻¹)

c. Working range (ng mL⁻¹)

Table. 5 Analysis of real sample with AALLME

| Sample | Added Pb ²⁺ (µg L ⁻¹) | Found ^a Pb ²⁺ (µg L ⁻¹) | Relative Recovery (%) |
|-------------|----------------------------------------------|-----------------------------------------------------------|-----------------------|
| River water | 0 | 8.4±0.4 | - |
| | 15 | 22.3 ± 1.1 | 92.6 |
| | 60 ^b | 66.3 ± 3.2 | 96.5 |
| Tap water | 0 | 4.1±0.2 | - |
| | 15 | 17.5 ± 0.9 | 89.3 |
| | 60 ^b | 62.2 ± 3.0 | 96.8 |
| Well water | 0 | 11.3 ± 0.6 | - |
| | 15 | 25.3 ± 1.5 | 93.3 |
| | 60 | 65.6 ± 3.7 | 90.5 |

^a Mean ± standard deviation (*n* = 3)^b Out of linear range

Table. 6. Determination of lead in geological certified reference material using proposed procedure.

| | Certified($\mu\text{g L}^{-1}$) | founded($\mu\text{g L}^{-1}$) | Recovery(%) |
|------|-----------------------------------|---------------------------------|-------------|
| JR-1 | 19.3 \pm 2.0 | 18.1 \pm 1.1* | 93.7 |

* Standard deviation (confidence interval 95 % , n=3)

1
2
3
4
5
6
7
8
9
10
11
12
13
14
15
16
17
18
19
20
21
22
23
24
25
26
27
28
29
30
31
32
33
34
35
36
37
38
39
40
41
42
43
44
45
46
47
48
49
50
51
52
53
54
55
56
57
58
59
60

